

DOI: 10.1002/adma.200700891

A Facile Synthesis of SmCo₅ Magnets from Core/Shell Co/Sm₂O₃ Nanoparticles**

By Yanglong Hou, Zhichuan Xu, Sheng Peng, Chuanbing Rong, J. Ping Liu, and Shouheng Sun*

The fabrication of SmCo-based nanomagnets exhibiting large coercivity and high magnetic moment has been a recent goal for materials research owing to the potential applications of these nanomagnets in high-performance permanent magnets and high-density data storage media.^[1–6] SmCo₅ is one of the most important hard magnetic materials in the SmCo alloy system. This material adopts a hexagonal close-packed (hcp) structure with Co and Co+Sm present in alternating layers along the *c*-axis, as shown in Figure 1. The easy magnetization direction of SmCo₅ is aligned along the *c*-direction of the lattice, and the magnetocrystalline anisotropy constant

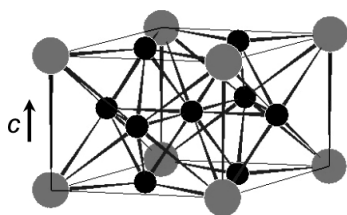
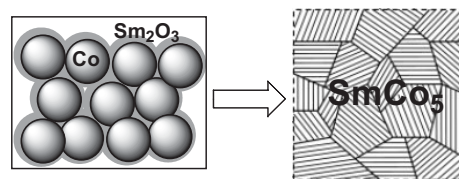


Figure 1. A hcp unit cell of the SmCo₅ alloy.

ranges from $1.1\text{--}2.0 \times 10^8 \text{ erg cm}^{-3}$ ($1 \text{ erg cm}^{-3} = 0.1 \text{ J m}^{-3}$); these values are among the highest known for hard magnetic materials.^[7–10] Furthermore, this alloy exhibits a very high Curie temperature ($T_c = 1020 \text{ K}$), which makes it superior to other classes of permanent magnetic materials, such as FePt ($T_c = 750 \text{ K}$) and Nd₂Fe₁₄B ($T_c = 585 \text{ K}$), for high-temperature applications.^[11–14] However, as with other rare-earth metal materials, metallic SmCo₅ nanoparticles are prone to fast oxidation. This chemical instability has made the synthesis of nanostructured SmCo₅ extremely difficult. Ball milling and melt spinning, the two standard physical methods used for the fabrication of nanostructured SmCo₅ magnets, provide only

limited control of the sizes of the final magnetic grains.^[15–23] Solution-phase chemical synthesis approaches have been applied to prepare monodisperse magnetic nanoparticles, and have recently been extended to the synthesis of SmCo₅ nanoparticles by coupling the polyol reduction of samarium acetylacetonate, Sm(acac)₃, with the thermal decomposition of Co₂(CO)₈.^[24–27] Although the molar ratio of Sm/Co in the two-component nanoparticles can be tailored to reach 1:5, there is no conclusive evidence that hcp-structured SmCo₅ is formed and that hard magnetic properties are obtained for the alloy nanoparticles.

Here, we report a facile synthesis of SmCo₅ magnets by the high-temperature reductive annealing of core/shell-structured Co/Sm₂O₃ nanoparticles. The nanocrystalline SmCo₅ particles adopt a hcp structure with a coercivity value as high as 24 kOe ($1 \text{ kOe} = 0.08 \text{ A m}^{-1}$) at 100 K and 8 kOe at room temperature. The synthesis is outlined in Scheme 1. The core/shell Co/Sm₂O₃ nanoparticles have been prepared by coating monodisperse Co nanoparticles with Sm₂O₃. The core/shell particles are reductively annealed in the presence of metallic



Scheme 1. Schematic illustration of the synthesis of nanocrystalline SmCo₅ by the reductive annealing of core/shell-structured Co/Sm₂O₃ nanoparticles.

Ca at 900 °C to reduce Sm₂O₃ to Sm and promote interface diffusion between Co and Sm. KCl has been used as a dispersion medium to facilitate the complete reduction of Sm₂O₃ and to prevent SmCo₅ from growing into a single crystal under the high-temperature annealing conditions. Nanocrystalline Sm₂CO₁₇ has also been prepared by annealing Co/Sm₂O₃ particles with a thicker Sm₂O₃ coating. This combination of solution-phase synthesis and solid-state high-temperature reduction offers a unique approach for the preparation of hard-magnetic nanocrystalline SmCo materials. Moreover, the process can be readily extended to fabricate SmCo₅–Co (or SmCo₅–CoFe) exchange-spring nanocomposites via the self-assembly of Co/Sm₂O₃ and Co (or CoFe₂O₄) nanoparti-

[*] Prof. S. Sun, Dr. Y. Hou, Z. Xu, S. Peng
Department of Chemistry, Brown University
Providence, RI 02912 (USA)
E-mail: ssun@brown.edu

Dr. C. Rong, Prof. J. P. Liu
Department of Physics, University of Texas at Arlington
Arlington, TX 76019 (USA)

[**] Y. Hou and Z. Xu contributed equally to this work. This work was supported by ONR/MURI under Grant No. N00014-05-1-0497.

cles. Such nanocomposites exhibit very large coercivity and magnetic moment values, which make them ideal for high-performance permanent magnet applications.^[28–32]

Co nanoparticles have been synthesized by the decomposition of $\text{Co}_2(\text{CO})_8$ in the presence of oleic acid and dioctylamine in 1,2,3,4-tetrahydronaphthalene (tetralin) at 210°C .^[33–35] Monodisperse 8 nm Co nanoparticles with a polycrystalline structure are obtained and dispersed in hexane. Figure 2a shows transmission electron microscopy (TEM) images of the Co nanoparticles used in this work. The

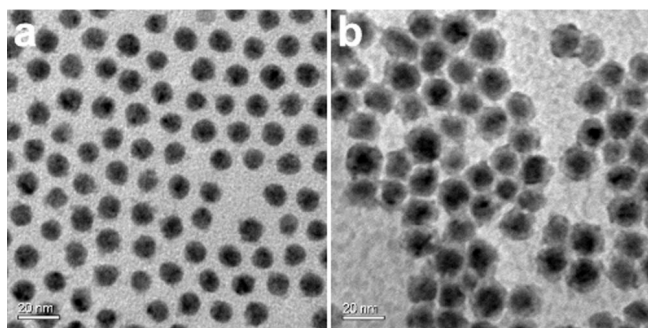


Figure 2. Transmission electron microscopy images of a) 8 nm Co nanoparticles and b) $\text{Co}/\text{Sm}_2\text{O}_3$ nanoparticles.

core/shell-structured $\text{Co}/\text{Sm}_2\text{O}_3$ nanoparticles have been prepared by the decomposition of $\text{Sm}(\text{acac})_3$ over the surface of the Co nanoparticles. In this coating process, $\text{Sm}(\text{acac})_3$ is first dissolved in oleylamine and oleic acid at 100°C . Subsequently, a hexane dispersion of Co nanoparticles is added into the $\text{Sm}(\text{acac})_3$ solution. The core/shell $\text{Co}/\text{Sm}_2\text{O}_3$ nanoparticles are prepared by heating the mixture to 250°C at a rate of 2°C min^{-1} . The composition of the particles has been determined by energy dispersive spectroscopy (EDS) and inductively coupled plasma-atomic emission spectroscopy (ICP-AES). By adjusting the relative amounts of $\text{Sm}(\text{acac})_3$ (1, 0.5, and 0.25 mmol) and Co nanoparticles (80 mg), Sm/Co molar ratios of 1:4.3, 1:5.2, and 1:7.5, respectively, have been obtained for the $\text{Co}/\text{Sm}_2\text{O}_3$ nanoparticles. Figure 2b shows a TEM image of core/shell-structured $\text{Co}/\text{Sm}_2\text{O}_3$ nanoparticles with a Sm/Co molar ratio of 1:4.3. The average thickness of the Sm_2O_3 shell is 2 nm. The selected area electron diffraction (SAED) pattern of these particles indicates that the Sm_2O_3 coating is amorphous. This is further corroborated by high-resolution TEM (HRTEM) images of the core/shell particles.

The structure of the core/shell $\text{Co}/\text{Sm}_2\text{O}_3$ nanoparticles has been further characterized by X-ray diffraction (XRD). The as-synthesized particles show only a broad diffraction peak at 44° , as shown in Figure 3a. This broad diffraction peak arises from the (111) plane of polycrystalline face-centered cubic (fcc) Co. Thermal annealing under an Ar atmosphere leads to the crystallization of the Co core (Fig. 3b–e). However, the Sm_2O_3 shell does not crystallize until an annealing tempera-

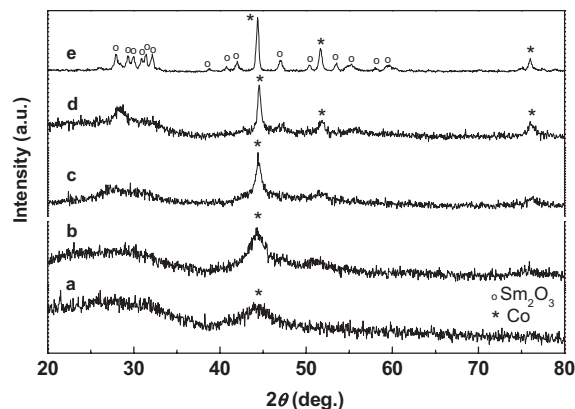


Figure 3. XRD patterns of a) $\text{Co}/\text{Sm}_2\text{O}_3$ nanoparticles (Sm/Co in a molar ratio of 1:4.3) and particles annealed under Ar at b) 450°C , c) 600°C , d) 750°C , and e) 900°C for 2 h. The Co and Sm_2O_3 phases in (e) match well with the standard fcc pattern of Co (Joint Committee on Powder Diffraction Standards (JCPDS) No. 89-4307) and bcc structure of Sm_2O_3 (JCPDS No. 25-0749).

ture of 750°C (Fig. 3d). At 900°C , both Co and Sm_2O_3 are well crystallized, as evidenced by the distinct diffraction peaks arising from both fcc Co and base-centered monoclinic (bcm) Sm_2O_3 (Fig. 3e). The diffraction pattern shown in Figure 3e further proves that there are no obvious chemical changes for the metallic Co under the 900°C annealing conditions. The diffraction patterns also corroborate the nanometer-sized structure of the Co core and Sm_2O_3 shell.

The core/shell-structured $\text{Co}/\text{Sm}_2\text{O}_3$ nanoparticles serve as the starting materials for the synthesis of SmCo_5 magnets under reductive annealing conditions. The reductive annealing has been performed under $\text{Ar} + 5\% \text{H}_2$ at a temperature of 900°C in the presence of metallic Ca. KCl with a melting point of 771°C is used as an inorganic solvent to ensure the complete reduction of Sm_2O_3 in the core/shell structure and to promote interface diffusion between Sm and Co. KCl is chosen over NaCl, a salt used in the synthesis of ferromagnetic FePt nanoparticles,^[36,37] since NaCl may get reduced under the current strongly reducing conditions. KCl may also act as a physical barrier to prevent the SmCo_5 magnets from growing into single crystals. Of the annealing parameters tested (annealing temperatures ranging from 700 to 1100°C and annealing times from 30 min to 2 h), annealing at 900°C for 1.5 h has been found to be ideal for the reduction of Sm_2O_3 and the formation of SmCo_5 . The Sm/Co composition of the nanomagnets obtained from the starting $\text{Co}/\text{Sm}_2\text{O}_3$ core/shell particles (Sm/Co in a molar ratio of 1:4.3) has been determined by EDS and ICP-AES to be 1:5. This ratio is slightly reduced from the starting particles, indicating that a small amount of Sm is lost during the annealing and/or subsequent washing processes.

The XRD pattern of the product obtained by the reductive annealing of the core/shell particles indicates the complete reduction of Sm_2O_3 and the formation of SmCo_5 , as shown in Figure 4a. The diffraction peaks match well with the standard

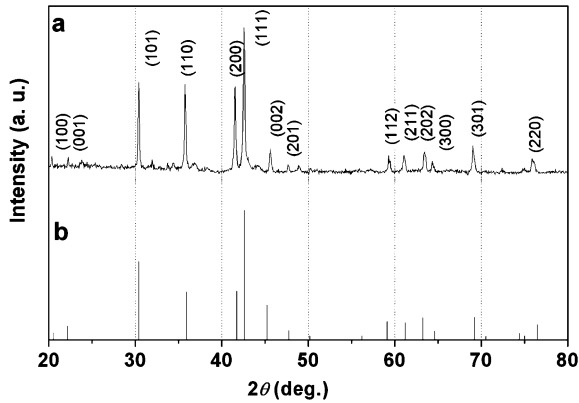


Figure 4. a) XRD pattern of nanocrystalline SmCo_5 prepared by the reductive annealing of $\text{Co}/\text{Sm}_2\text{O}_3$ nanoparticles; b) the standard diffraction pattern of hcp-structured SmCo_5 (JPCDS No. 65-8981).

SmCo_5 pattern (Joint Committee on Powder Diffraction Standards (JCPDS) No. 65-8981, Fig. 4b), indicating that high-temperature reduction and interface diffusion lead to the formation of hcp-structured SmCo_5 . The correlated SmCo_5 crystal size estimated from the (200) diffraction peak using Scherrer's formula is around 32 nm. Figure 5a shows a HRTEM image of a typical assembly of SmCo_5 magnets. It can be seen that the nanoscale domains adopt different structural orienta-

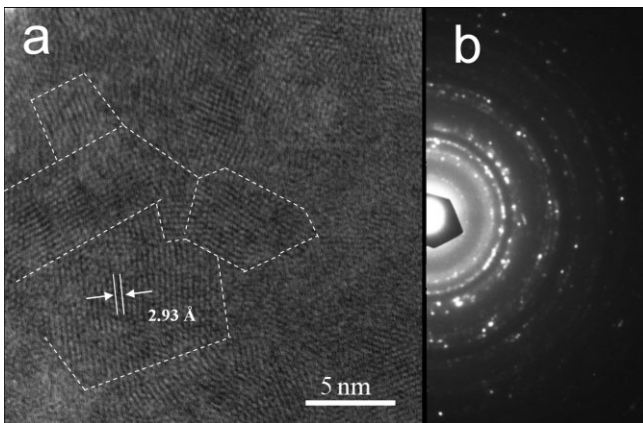


Figure 5. a) HRTEM image of an assembly of nanocrystalline SmCo_5 structures with the dashed lines indicating the nanocrystalline grain boundaries, and b) SAED pattern of nanocrystalline SmCo_5 .

tions. The lattice fringes within each crystal domain have an interfringe spacing of 2.93 Å. This spacing is close to the interplane distance of 2.91 Å between the (101) planes in hcp-structured SmCo_5 . Figure 5b shows the SAED pattern of the SmCo_5 product. The ring pattern arises from the 3D random orientation of nanometer-sized grains within the structure.

The core/shell $\text{Co}/\text{Sm}_2\text{O}_3$ nanoparticles are superparamagnetic. After reductive annealing, the nanocrystalline SmCo_5 becomes strongly ferromagnetic. Figure 6 shows the hysteresis

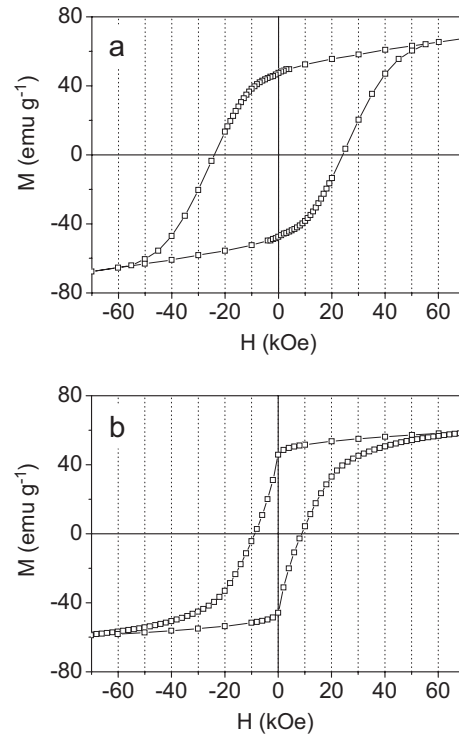


Figure 6. Hysteresis loops of nanocrystalline SmCo_5 measured at a) 100 K and b) 300 K.

loops of the SmCo_5 magnets measured using a superconducting quantum interference device (SQUID). It can be seen that the coercivity of the magnets reaches 24 kOe at 100 K (Fig. 6a) and 8 kOe at room temperature (Fig. 6b) with a remnant magnetic moment of 40–50 emu g^{-1} ($1 \text{ emu g}^{-1} = 1 \text{ A m}^2 \text{ kg}^{-1}$). It is worth noting that when core/shell nanoparticles with a thicker Sm_2O_3 coating (Sm/Co in a ratio of 1:7.5) are used as precursors, nanocrystalline $\text{Sm}_2\text{Co}_{17}$ is obtained. The room-temperature hysteresis loop of the $\text{Sm}_2\text{Co}_{17}$ magnets show a smaller coercivity value of 1.4 kOe, but exhibit a higher saturation moment of 70 emu g^{-1} , indicating that the doping of high amounts of Co in $\text{Sm}_2\text{Co}_{17}$ particles leads to a decrease of the magnetocrystalline anisotropy and an increase of the magnetic moment. This is consistent with previous observations of SmCo alloy materials.

In summary, we have developed a novel procedure to make hard-magnetic nanocrystalline SmCo_5 (or $\text{Sm}_2\text{Co}_{17}$) particles from core/shell-structured $\text{Co}/\text{Sm}_2\text{O}_3$ nanoparticles by high-temperature reductive annealing. The nanostructured magnets have a well-controlled crystal morphology, and their magnetic coercivity can be as high as 24 kOe at 100 K and 8 kOe at room temperature. This synthesis represents an important first step for fabricating air-stable SmCo -based nanoparticles and nanocomposite magnets. We are currently developing self-assembly and reductive annealing approaches for the preparation of SmCo_5 -Co and SmCo_5 -CoFe exchange-spring nanocomposite magnets.

Experimental

Sm(acac)₃, tetralin (99%), oleic acid (90%), oleylamine (70%), and dioctylamine (98%) were purchased from Aldrich. Co₂(CO)₈ was obtained from Strem. These chemicals were used without further purification.

Synthesis of 8 nm Co Nanoparticles: 0.3 mL of oleic acid and 0.5 mL of dioctylamine were dissolved in 20 mL of tetralin by heating at 100 °C for 1 h under a nitrogen atmosphere. The mixture was then cooled to room temperature. Subsequently, 0.54 g of Co₂(CO)₈ was quickly added into the solution. The solution was then heated up to 100 °C for 30 min and subsequently to 210 °C for 20 min, before cooling down to room temperature. The Co nanoparticles were precipitated by adding 20 mL ethanol and washed three times with ethanol. The as-prepared Co nanoparticles were then dispersed in hexane.

Synthesis of Core/Shell-Structured Co/Sm₂O₃ Nanoparticles: Sm(acac)₃ (1 mmol) was dissolved in a mixture of 10 mL oleylamine and 1 mL oleic acid. The solution was degassed at 120 °C for 1 h. 8 nm Co nanoparticles (80 mg) in 5 mL hexane were then added into the solution. The solution was kept at 120 °C for 1 h to remove hexane. Subsequently, the mixture was heated to 250 °C at a heating rate of 2 °C min⁻¹ and kept at this temperature for 4 h before cooling down to room temperature. The Co/Sm₂O₃ nanoparticles (Sm/Co in a molar ratio of 1:4.3) were precipitated by ethanol and separated by centrifuging at 8000 rpm for 6 min. The as-prepared core/shell nanoparticles were dispersed in hexane for further characterization.

The molar ratio of Sm/Co in the Co/Sm₂O₃ nanoparticles was controlled by changing the ratio of Sm(acac)₃ to Co nanoparticles. For example, core/shell nanoparticles with Sm/Co molar ratios of 1:7.5, 1:5.2, and 1:4.3 were synthesized by using 0.25, 0.5, and 1 mmol of Sm(acac)₃, respectively, along with 80 mg of Co nanoparticles.

Synthesis of SmCo₅ Magnets: In a typical procedure for the synthesis of SmCo₅ nanomagnets, 200 mg of Co/Sm₂O₃ (Sm/Co in a molar ratio of 1:4.3) nanoparticles were mixed with 90 mg of KCl. 300 mg of Ca powder was ground together with the nanoparticles and KCl under an Ar atmosphere. The mixture was then quickly transferred to a quartz tube that had been flushed with Ar + 5% H₂. The tube was heated to 100 °C for 30 min to remove traces of moisture and air adsorbed on the walls of the tube, and then subsequently to 900 °C at a rate of 20 °C min⁻¹. The reaction mixture was then held at 900 °C for 1.5 h. Subsequently, the tube was allowed to cool down to room temperature by turning off the power of the furnace. The product was washed with degassed distilled water under N₂ to dissolve CaO, KCl, and extra Ca. The powder was further washed with degassed ethanol and dried under vacuum at room temperature for further characterization. 50 mg of the magnetic product was obtained in a typical run. Similarly, Sm₂Co₁₇ magnets were prepared by the reductive annealing of Co/Sm₂O₃ nanoparticles with a Sm/Co ratio of 1:7.5.

Nanomagnet Characterization: The size and morphology of the nanoparticles were characterized using Philips EM 420 (120 kV) and JEOL 2010 (200 kV) instruments. Powder XRD patterns of the samples were recorded on a Bruker AXS D8-Advanced diffractometer with CuK α radiation ($\lambda = 1.5418 \text{ \AA}$). Magnetic studies were performed using a Quantum Design SQUID instrument with a field up to 70 kOe. The compositions of the samples were characterized by Oxford EDS and ICP-AES.

Received: April 14, 2007

Revised: June 5, 2007

Published online: September 25, 2007

[1] M. Hasegawa, K. Uchida, Y. Nozawa, M. Endoh, S. Tanigawa, S. G. Sankar, M. Tokunaga, *J. Magn. Magn. Mater.* **1993**, *124*, 325.
 [2] T. Budde, H. H. Gatzel, *J. Magn. Magn. Mater.* **2004**, *272–276*, 2027.
 [3] E. Pina, F. J. Palomares, M. A. Garcia, F. Cebollada, A. de Hoyos, J. J. Romero, A. Hernando, J. M. Gonzalez, *J. Magn. Magn. Mater.* **2005**, *290*, 1234.

[4] J. Sayama, K. Mizutani, Y. Yamashita, T. Asahi, T. Osaka, *IEEE Trans. Magn.* **2005**, *41*, 3133.
 [5] H. Raisigel, O. Cugat, J. Delamare, *Sens. Actuators A* **2006**, *130*, 438.
 [6] T. Budde, H. H. Gatzel, *J. Appl. Phys.* **2006**, *99*, 08N304.
 [7] K. J. Strnat, in *Ferromagnetic Materials* (Eds: E. P. Wohlfarth, K. H. J. Buschow), Vol. 4, North-Holland, Amsterdam **1988**, p 131.
 [8] S. A. Majetich, E. M. Kirkpatrick, *IEEE Trans. Magn.* **1997**, *33*, 3721.
 [9] P. Larson, I. I. Mazin, D. A. Papaconstantopoulos, *Phys. Rev. B: Condens. Matter* **2003**, *67*, 214405.
 [10] J. Fidler, T. Schrefl, W. Scholz, D. Suess, R. Dittrich, M. Kirschner, *J. Magn. Mater.* **2004**, *272–276*, 641.
 [11] O. Gutfleisch, J. Lyubina, K.-H. Müller, L. Schultz, *Adv. Eng. Mater.* **2005**, *7*, 208.
 [12] T. Schrefl, J. Fidler, W. Scholz, *IEEE Trans. Magn.* **2000**, *36*, 3394.
 [13] I. A. Al-Omari, R. Skomski, R. A. Thomas, D. Leslie-Pelecky, D. J. Sellmyer, *IEEE Trans. Magn.* **2001**, *37*, 2534.
 [14] C. B. Rong, H. W. Zhang, R. J. Chen, B. G. Shen, S. L. He, *J. Appl. Phys.* **2006**, *100*, 123913.
 [15] J. Ding, P. G. McCormick, R. Street, *J. Alloys Compd.* **1995**, *228*, 102.
 [16] S. K. Chen, J. L. Tsai, T. S. Chin, *J. Appl. Phys.* **1996**, *79*, 5964.
 [17] E. M. Kirkpatrick, D. L. Leslie-Pelecky, *J. Appl. Phys.* **2000**, *87*, 6734.
 [18] K. Gallagher, M. Venkatesan, J. M. D. Coey, *IEEE Trans. Magn.* **2001**, *37*, 2528.
 [19] L. Li, W. Y. Zhang, Y. Q. Zhou, J. Q. Li, B. G. Shen, J. Zhang, *Appl. Phys. Lett.* **2002**, *80*, 2660.
 [20] J. Zhou, R. Skomski, D. J. Sellmyer, *J. Appl. Phys.* **2003**, *93*, 6495.
 [21] A. Hsiao, S. Aich, L. H. Lewis, J. E. Shield, *IEEE Trans. Magn.* **2004**, *40*, 2913.
 [22] V. M. Chakka, B. Altuncavahir, Z. Q. Jin, Y. Li, J. P. Liu, *J. Appl. Phys.* **2006**, *99*, 08E912.
 [23] V. Pop, O. Isnard, I. Chichinas, D. Givord, J. M. Le Breton, *J. Optoelectron. Adv. Mater.* **2006**, *8*, 494.
 [24] K. Ono, Y. Kakefuda, R. Okuda, Y. Ishii, S. Kamimura, A. Kitamura, M. Oshima, *J. Appl. Phys.* **2002**, *91*, 8480.
 [25] H. W. Gu, B. Xu, J. C. Rao, R. K. Zheng, X. X. Zhang, K. K. Fung, C. Y. C. Wong, *J. Appl. Phys.* **2003**, *93*, 7589.
 [26] X. Teng, H. Yang, *J. Nanosci. Nanotechnol.* **2007**, *7*, 356.
 [27] J. H. Hong, W. S. Kim, J. I. Lee, N. H. Hur, *Solid State Commun.* **2007**, *141*, 541.
 [28] R. F. Sabiryanov, S. S. Jaswal, *Phys. Rev. B: Condens. Matter* **1998**, *58*, 12071.
 [29] J. P. Liu, Y. Liu, R. Skomski, D. J. Sellmyer, *J. Appl. Phys.* **1999**, *85*, 4812.
 [30] J. Sort, S. Surinach, J. S. Munoz, M. D. Baro, J. Nogues, G. Chouteau, V. Skumryev, G. C. Hadjipanayis, *Phys. Rev. B: Condens. Matter* **2002**, *65*, 174420.
 [31] J. E. Davies, O. Hellwig, E. E. Fullerton, J. S. Jiang, S. D. Bader, G. T. Zimanyi, K. Liu, *Appl. Phys. Lett.* **2005**, *86*, 262503.
 [32] J. S. Jiang, J. E. Pearson, Z. Y. Liu, B. Kabius, S. Trasobares, D. J. Miller, S. D. Bader, D. R. Lee, D. Haskel, G. Srarjer, J. P. Liu, *J. Appl. Phys.* **2005**, *97*, 10K311.
 [33] V. F. Puentes, K. M. Krishnan, A. P. Alivisatos, *Science* **2001**, *291*, 2115.
 [34] V. F. Puentes, K. M. Krishnan, A. P. Alivisatos, *Appl. Phys. Lett.* **2001**, *78*, 2187.
 [35] Y. Bao, M. Beerman, A. B. Pakhomov, K. M. Krishnan, *J. Phys. Chem. B* **2005**, *109*, 7220.
 [36] K. Elkins, D. Li, N. Poudyal, V. Nandwana, Z. Jin, K. Chen, J. P. Liu, *J. Phys. D: Appl. Phys.* **2005**, *38*, 2306.
 [37] J. P. Liu, K. Elkins, D. Li, V. Nandwana, N. Poudyal, *IEEE Trans. Magn.* **2006**, *42*, 3036.